Exchange between the upper tropical troposphere and the lower stratosphere studied with aircraft observations

A. F. Tuck,[1] S. J. Hovde,[1,2] K. K. Kelly,[1] M. J. Mahoney,[3] M. H. Proffitt,[4] E. C. Richard[1,2] and T. L. Thompson[1]

Received 10 January 2003; revised 12 August 2003; accepted 27 August 2003; published 11 December 2003.

[1] Exchange between the upper tropical troposphere and the lower stratosphere is considered by examining WB57F and ER-2 aircraft observations of water, ozone, wind, and temperature in the potential temperature range $360 < \theta < 420$ K. These processes are examined in part by using the technique of unified scale invariance on the airborne data, as has been done previously for the lower stratospheric polar vortex. Scale invariance is found, on scales from a few hundred meters to the maximum flown, 2700 km (25 great circle degrees). The results apply both to vertical exchange at the tropical tropopause and to isentropic exchange at the subtropical jet stream. All scales participate in the maintenance of the mean state, with substantial contributions from relatively infrequent but intense events in the long tails of the probability distributions. Past data are examined and found to fit this general framework. A unique mapping of tropical tropopause temperature to the total hydrogen content of the middleworld and overworld should not be expected; the head of the "tape recorder" is at 50–60 hPa rather than 90–100 hPa. The tropical tropopause is observed at potential temperatures θ_T greater than the maximum moist static surface values θ_W, such that $\theta_T - \theta_W$ varies between 10 K in fall and up to 40 K in spring. The meridional gradient of θ_T is directed from the subtropical jet stream to the inner tropics, with θ_T declining by approximately 10 K from near 30°N to near 10°N in the vicinity of 95°W. The maintenance of these θ_T values is discussed. Total water (measured as the sum of vapor and vaporized ice) and ozone, major absorbers of solar radiation and emitters/absorbers of terrestrial infrared radiation, show scale invariance in the upper tropical troposphere. The implications of this result for the notion of a conservative cascade of energy via fluid dynamics from the largest to the smallest scales are discussed. The scaling exponents H_z for total water and ozone in the upper tropical troposphere are not the value, 5/9, expected for a passive scalar, probably indicating the presence of sources and/or sinks operating faster than mixing. *INDEX TERMS:* 0340 Atmospheric Composition and Structure: Middle atmosphere—composition and chemistry; 3250 Mathematical Geophysics: Fractals and multifractals; 3362 Meteorology and Atmospheric Dynamics: Stratosphere/troposphere interactions; *KEYWORDS:* upper tropical troposphere, multifractal

Citation: Tuck, A. F., S. J. Hovde, K. K. Kelly, M. J. Mahoney, M. H. Proffitt, E. C. Richard, and T. L. Thompson, Exchange between the upper tropical troposphere and the lower stratosphere studied with aircraft observations, *J. Geophys. Res.*, *108*(D23), 4734, doi:10.1029/2003JD003399, 2003.

1. Introduction

[2] The Brewer-Dobson circulation [*Brewer*, 1949] has been the main conceptual framework in which the entry of air to the stratosphere has been examined; it has stood the test of time as a zonally and temporally averaged construct for the tracer content and the drying of air transported into the stratosphere from the tropical troposphere. It is of course a global scale mechanism, involving a zonal average over all longitudes. The view offered by the direct interpretation of in situ aircraft observations revealed considerable structure both in the vertical and horizontal [*Tuck et al.*, 1997] and demonstrated the importance of smaller scales. The scale of the transport mechanisms involved has been an important thread; it was implicitly global in the original formulation, a view recently reiterated [*Dessler*, 1998], and has ranged from the consideration of individual thunderstorms (≈10 km scale) [*Johnston and Solomon*, 1979] to the "stratospheric fountain" (≈100° longitude scale) [*Newell and Gould-Stewart*, 1981].

[3] Recently, there has been consideration of the role of cirrus decks [*Jensen et al.*, 1996], monsoon convection

[1]Aeronomy Laboratory, National Oceanic and Atmospheric Administration, Boulder, Colorado, USA.
[2]Cooperative Institute for Research in Environmental Science, University of Colorado, Boulder, Colorado, USA.
[3]Jet Propulsion Laboratory, California Institute of Technology, Pasadena, California, USA.
[4]World Meteorological Organization, Geneva, Switzerland.

0148-0227/03/2003JD003399$09.00

Table 1. Flight Segments Used in the Scaling Analysis

Aircraft	Date, year/month/day	Segment Duration, s	Coordinates (latitude, longitude)	Segment Center Time, UTCs	Approximate Mean θ, K
ER-2	870203	6971	(14°S, 129°E) (18°S, 117°E)	91,635	412
ER-2	870814	6845	(7°N, 79°W) (5°S, 78°W)	48,470	391
ER-2	941026	8207	(15°N, 158°W)(1°N, 159°W)	76,878	410
WB57F	980409	7017	(28°N, 93°W) (17°N, 84°W)	59,534	368
WB57F	980409	5943	(19°N, 85°W) (27°N, 91°W)	66,911	413
WB57F	980501	8209	(28°N, 94°W) (14°N, 95°W)	57,962	362
WB57F	980501	7242	(13°N, 95°W) (26°N, 95°W)	66,259	370
WB57F	980504	7926	(14°N, 95°W) (28°N, 95°W)	68,442	420
WB57F	980507	5144	(30°N, 93°W) (33°N, 83°W)	56,910	373
WB57F	980511	8872	(28°N, 95°W) (11°N, 95°W)	58,357	374
WB57F	980511	8052	(13°N, 95°W) (28°N, 95°W)	67,906	418
WB57F	990920	13525	(28°N, 87°W) (5°N, 94°W)	46,669	362
WB57F	990921	10992	(13°N, 82°W) (28°N, 94°W)	68,936	360
WB57F	20020726	3125	(22°N, 86°W) (17°N, 84°W)	63,738	369

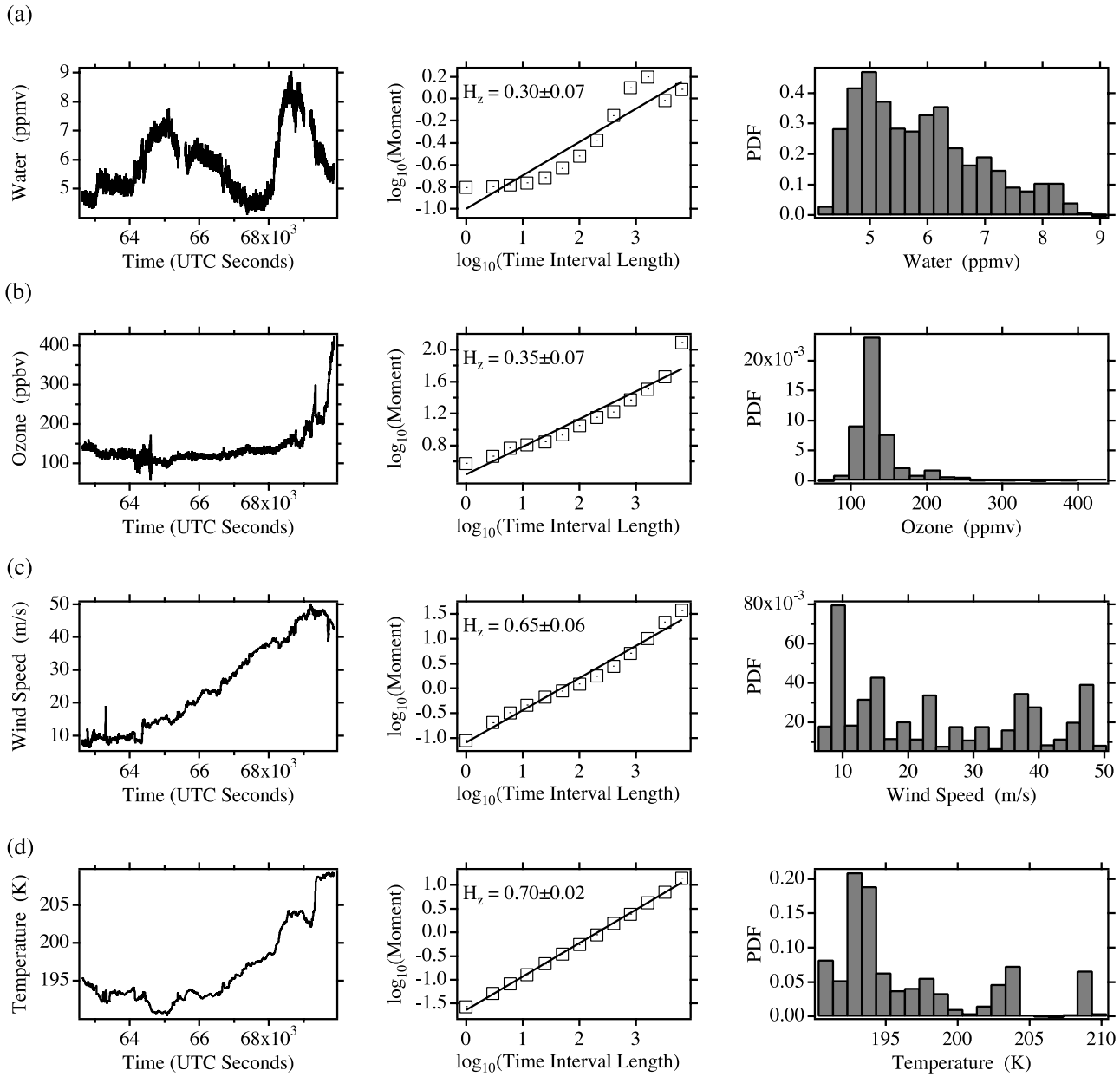

Figure 1. The instrumental time trace, the log-log plot for the estimation of H_z, and the associated histogram for the WB57F flight 7242-s in length (Table 1), 1 May 1998. (a) Water, (b) ozone, (c) wind speed, and (d) temperature.

Table 2. Values of H_z Calculated From the Flight Segments in Table 1[a]

Segment Duration, s	$H_z(H_2O)$	$H_z(O_3)$	$H_z([u^2 + v^2]^{1/2})$	$H_z(T)$	Figure
6971	...	0.34 ± 0.07	...	0.49 ± 0.03	
	0.13	0.34 ± 0.07	...	0.49 ± 0.04	
6845	...	...	0.35 ± 0.04	0.34 ± 0.04	4
	0.08 ± 0.23	0.19 ± 0.05	0.38 ± 0.02	0.38 ± 0.05	
8207	...	0.37 ± 0.04	0.49 ± 0.07	0.52 ± 0.02	
	0.10 ± 0.03	0.32 ± 0.04	0.58 ± 0.03	0.53 ± 0.02	
7017	...	...	0.56 ± 0.07	0.66 ± 0.02	14
	0.45 ± 0.23	0.24 ± 0.08	0.47 ± 0.04	0.64 ± 0.03	
5943	...	0.43 ± 0.05	0.36 ± 0.04	0.61 ± 0.03	14
	0.12 ± 0.06	0.42 ± 0.05	0.34 ± 0.04	0.61 ± 0.05	
8209	0.43 ± 0.05	0.51 ± 0.08	0.64 ± 0.06	0.65 ± 0.04	14
	0.54 ± 0.04	0.39 ± 0.06	0.56 ± 0.04	0.61 ± 0.04	
7242	0.30 ± 0.07	0.35 ± 0.07	0.65 ± 0.06	0.70 ± 0.02	1, 6, 14
	0.53 ± 0.16	0.27 ± 0.03	0.57 ± 0.05	0.68 ± 0.02	
7926	...	0.48 ± 0.10	0.36 ± 0.05	0.59 ± 0.03	14
	0.09 ± 0.03	0.34 ± 0.08	0.40 ± 0.03	0.58 ± 0.04	
5144	0.35 ± 0.05	0.51 ± 0.09	0.56 ± 0.03	...	13
	0.46 ± 0.04	0.41 ± 0.08	0.57 ± 0.03	0.57 ± 0.09	
8872	...	...	0.57 ± 0.06	0.65 ± 0.04	3, 14
	0.38 ± 0.05	0.20 ± 0.05	0.51 ± 0.06	0.60 ± 0.02	
8052	...	0.39 ± 0.05	0.43 ± 0.04	0.62 ± 0.03	3, 14
	0.10 ± 0.03	0.33 ± 0.04	0.41 ± 0.06	0.62 ± 0.04	
13,525	0.26 ± 0.04	0.37 ± 0.06	...	0.47 ± 0.09	14
	0.27 ± 0.04	0.31 ± 0.07	0.50 ± 0.11	0.59 ± 0.04	
10,992	0.31 ± 0.04	0.33 ± 0.04	0.48 ± 0.04	0.55 ± 0.04	5, 14
	0.37 ± 0.02	0.30 ± 0.05	0.46 ± 0.05	0.60 ± 0.04	
3125	0.39 ± 0.03	0.43 ± 0.05	...	0.47 ± 0.06	
	0.44 ± 0.03	0.44 ± 0.06	0.45 ± 0.08	0.47 ± 0.09	
Mean	0.34 ± 0.08	0.38 ± 0.09	0.50 ± 0.11	0.56 ± 0.10	
	0.29 ± 0.20	0.32 ± 0.09	0.48 ± 0.10	0.57 ± 0.09	

[a]The top number in each cell results from the line fit to the variogram across all scales. The bottom number results from fitting 1–1000 s in the case of ozone, temperature, and wind speed, and from the end of the instrument noise regime to 1000 s in the case of water. Errors are 95% confidence intervals. A missing error means that the line fit was determined by two points. The rightmost column references figures where appropriate.

[*Potter and Holton*, 1995], and of a posited reverse Walker cell in the Pacific lower stratosphere [*Gage et al.*, 1991; *Sherwood*, 2000]. *Danielsen* [1993] demonstrated irreversible transport of air across the tropopause by convective cloud turrets and larger scale upwelling in tropical cyclones north of Australia during January and February 1987. Earlier suggestions [*Brewer*, 1960; *Murgatroyd*, 1965; *Foot*, 1984; *Allam and Tuck*, 1984] of horizontal transport across the subtropical jet stream from the upper tropical troposphere to the lower midlatitude stratosphere have been supported by more recent work [*Dessler et al.*, 1995]. The subtropical jet stream has three isotach maxima in the Northern Hemisphere, centered at approximately 28°N in the zonal mean. Analysis of radar and ozone soundings in the context of potential vorticity maps has shown adiabatic transport from the subtropics into the lower midlatitude stratosphere at the potential temperatures of the subtropical jet stream, $345 < \theta < 400$ K [*Vaughan and Timmis*, 1998; *O'Connor et al.*, 1999]. *Dunkerton* [1995], *Rosenlof et al.* [1997], and *Dethof et al.* [1999] showed large-scale evidence for the transport of moist air across the subtropical jet stream in association with upper level monsoon anticyclones. Aircraft profiles of ozone, water, tracer, and particles showed unequivocally the intrusion of deep (≈4 km) layers of air from the tropics into the Northern Hemisphere midlatitude lower stratosphere in this altitude band and moreover that there was a significant increase in the frequency of occurrence of such ozone-poor, high-tracer intrusions in the 30-year ozonesonde record [*Reid et al.*, 2000]. The zonal length scale of these events can be thousands of kilometers. Such a transport mechanism offers a possible explanation for the increase in lower stratospheric water vapor abundance since the 1950s [*Rosenlof et al.*, 2001]. Because the mechanism bypasses the "cold trap" at the tropical tropopause, it can resolve the paradox of how stratospheric water content can have increased in the presence of a cooling trend at the tropical tropopause [*Simmons et al.*, 1999].

[4] The above mechanisms cover the range of scales from individual storm turrets to the Walker cell, approximately 10–10,000 km. Here we use unique data for 3 flight segments of the ER-2 and 11 from the WB57F (Table 1) to examine the scaling behavior [*Tuck and Hovde*, 1999a, 1999b; *Tuck et al.*, 1999] and probability distribution functions [*Sparling*, 2000] in water, methane, ozone, wind, and temperature in the range $360 < \theta < 420$ K at tropical and subtropical latitudes. The aircraft data uniquely cover the smaller scales, down to 200 m, as well as having horizontal flight segments up to 2700 km (25 great circle degrees) near the tropical tropopause. It is important to note that these data apply to a region in which in situ observations are scarce, despite its importance as the region where water vapor infrared absorption bands change from being optically thick below and optically thin above, giving it a central role in the radiative balance [*Doherty and Newell*, 1984].

[5] We apply the first-order structure function measure of generalized scale invariance H_z [*Schertzer and Lovejoy*, 1985; *Seuront et al.*, 1999; *Tuck et al.*, 2002] to observations of wind speed, temperature, ozone, and where possible to total water (vapor plus ice crystals detected as vapor) made

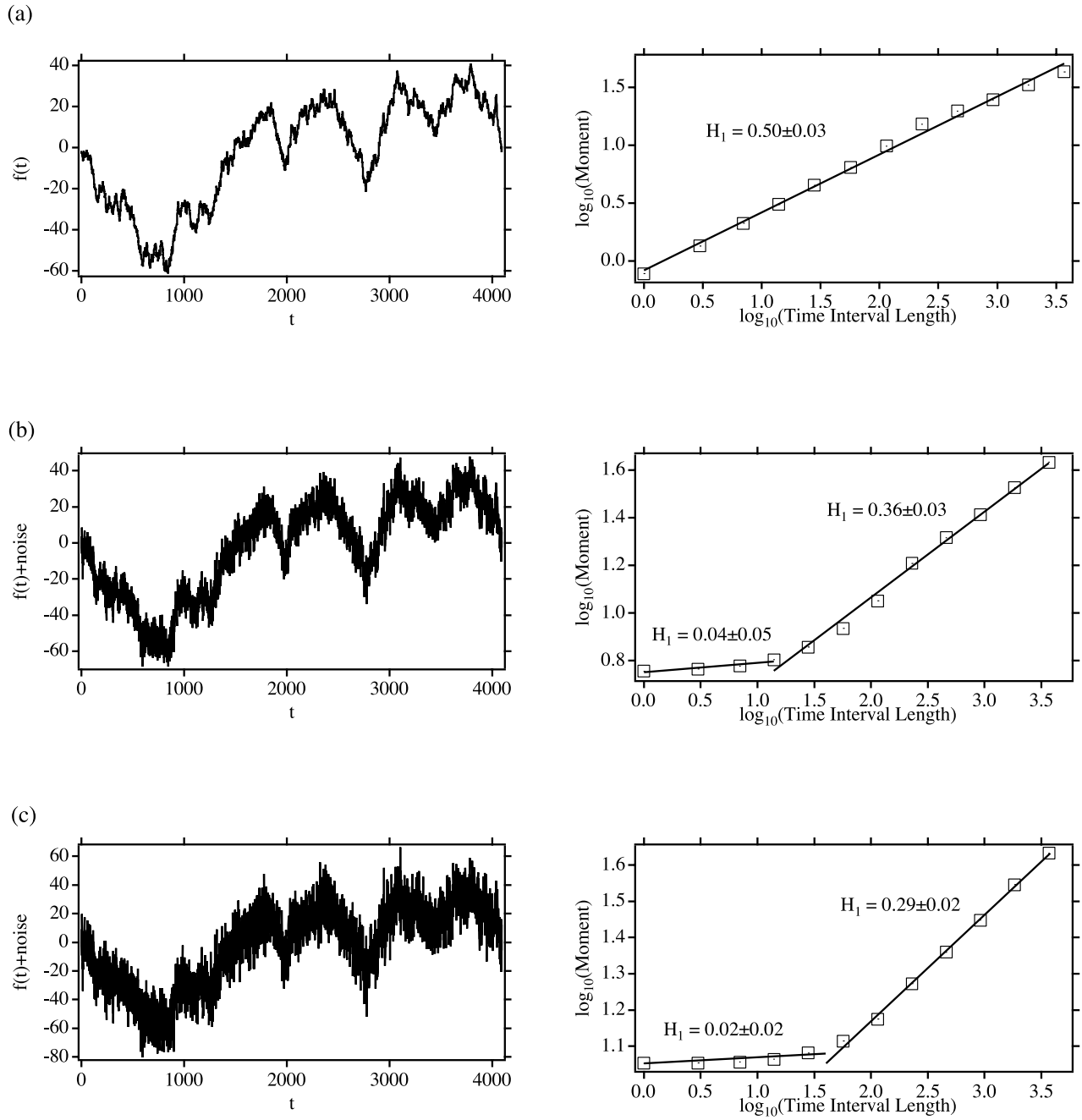

Figure 2. The effect of adding Gaussian noise on the scaling for a synthetically generated trace with $H_1 = 0.50 \pm 0.03$. (a) The ideal trace (left) and the log-log plot (right), (b) the equivalent diagrams with 5% noise added, and (c) the equivalent diagrams with 10% noise added.

at low latitudes from ER-2 and WB57F aircraft flying above, at and below the tropopause. The tropopause is defined as that observed by the Microwave Temperature Profiler (MTP) instrument on the aircraft [*Denning et al.*, 1989], using the WMO temperature lapse rate criterion. The results are used to gain insight into any scale dependence that might be evident in exchange of air between the troposphere and the stratosphere in the tropics and subtropics. The long-tailed distributions in stratospheric water vapor reported by *Helliwell et al.* [1957] and *Mastenbrook* [1968] are interpreted and confirmed in the light of modern results. Scale invariance generally will mean that all scales contribute and that a relatively small number of large amplitude events will have a substantial effect.

2. Method

[6] We select all approximately horizontal segments of all flights of ER-2 and WB57F aircraft since January 1987 which satisfy the following criteria: duration $\geq$3000 s and potential temperature $\theta \leq 420$ K, with the exception of flights over tropical cyclones and hurricanes (three in

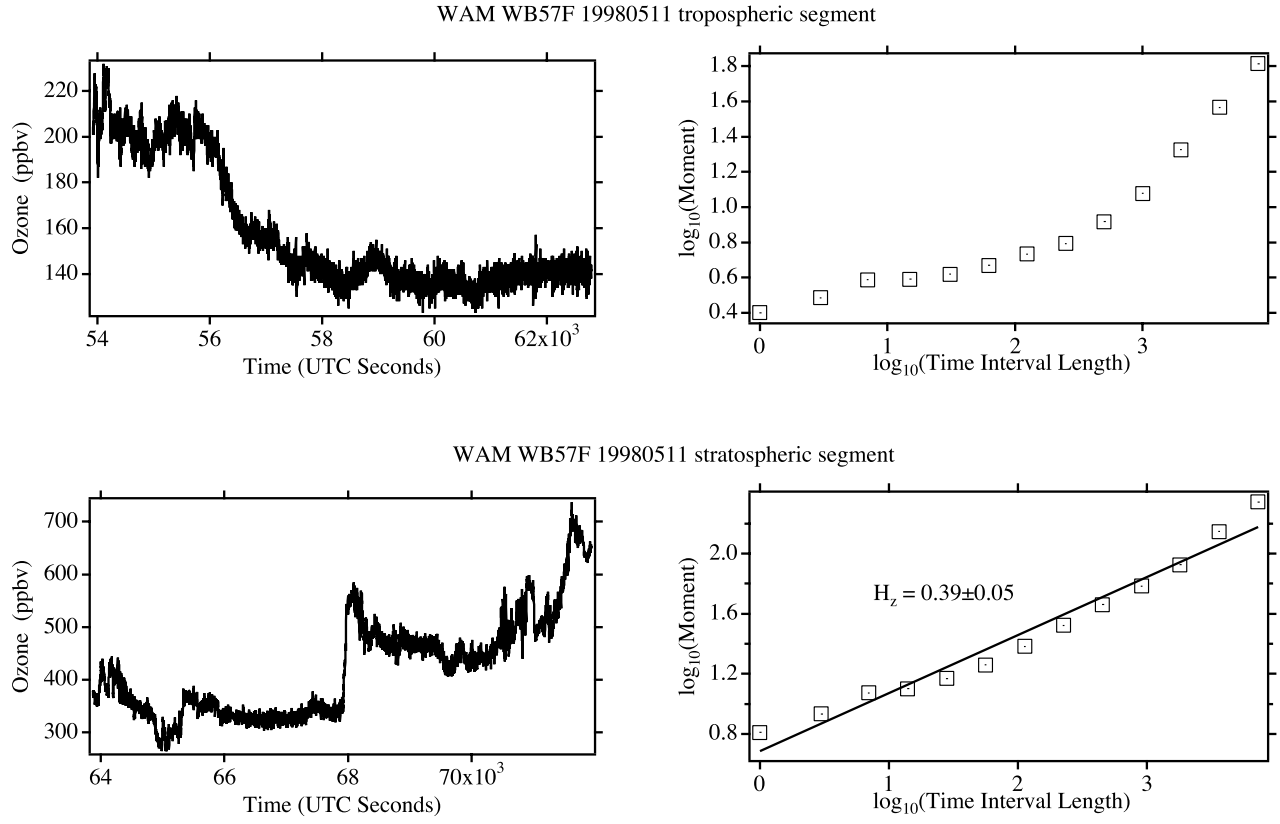

Figure 3. Illustration of scaling behavior for ozone during the flight of 11 May 1998. The stratospheric leg, where ozone mixing ratios are much higher than the instrumental noise, scales, whereas the upper tropospheric leg, with much lower ozone mixing ratios, does not.

number), at latitudes <35°. This yields 3 segments from 3 flights of the ER-2 and 11 segments from 8 flights of the WB57F. The flight segments are specified in Table 1. Both aircraft cruise at Mach 0.7 or very close to 200 m s^{-1} for the flights used here. All data were analyzed at 1 Hz.

[7] Some discussion of the effects of aircraft motion seems warranted. The autopilot often flies the aircraft in "Mach hold" mode when cruising at altitude, relieved as necessary by manual control from the cockpit. In Mach hold mode, the autopilot attempts to keep Mach number $M = {}^{a}v(\gamma RT)^{-0.5}$ constant, where ${}^{a}v$ is the speed of the aircraft, γ is the ratio of specific heats of dry air, R is the gas constant for dry air, and T is the absolute temperature. We will use an upper prefix "a" to refer to variables describing aircraft motion to distinguish them from those describing atmospheric motion. The actual three-dimensional flight path through the atmosphere is a reflection of how the autopilot control laws respond to atmospheric variations, and no vertical coordinate (altitude, pressure, and potential temperature) remains constant. One might for example seek to impose such constancy by selecting only those data points at a given, narrowly defined value of θ. The relation for θ is $\theta = T(1000/P)^{1-\gamma}$, where P is pressure in hPa. The control laws cited in aerodynamics texts [*Etkin*, 1972], for example, show highly nonlinear responses to velocity perturbations on all three axes, and we see no practical way of removing sampling biases caused by aircraft motion with respect to θ. In these circumstances, we have opted for analysis of what is actually observed, namely a time series at constant time interval over an approximately horizontal path with fluctuations in altitude, pressure, and potential temperature. It has been argued that such a time series will result in a scaling exponent H_z for wind speed, temperature, and passive scalars (tracers) of 5/9 or 0.555 [*Lovejoy et al.*, 2001; *Tuck et al.*, 2002, 2003], an hypothesis borne out by the data analysis in those references. This topic is discussed further below.

[8] Each flight segment was analyzed as described previously [*Tuck et al.*, 2002]. Here we consider total water, ozone, horizontal wind speed, and temperature. The exponent H_z was evaluated from the first-order structure function, as for the polar vortex data [*Tuck et al.*, 2002, 2003].

[9] All variables showed evidence for scale invariance during all the flight segments, provided their signal-to-noise was adequately larger than the atmospheric variability, as gauged by linear log-log plots. An example of a scale-invariant flight segment is shown in Figure 1 for each variable during the 7242-s long trace of the WB57F on 1 May 1998. This took place between (13°N, 95°W) and (26°N, 95°W) and was a flight path which followed the tropopause as accurately as possible, using real-time feedback from the MTP [*Denning et al.*, 1989]. Deviations of the aircraft from the tropopause altitude were generally less than 200 m. Since scale invariance is associated with long-tailed probability distributions [*Schertzer and Lovejoy*, 1987], histograms were produced for all variables along all flight segments in order to ascertain the existence of such tails (see Figure 1).

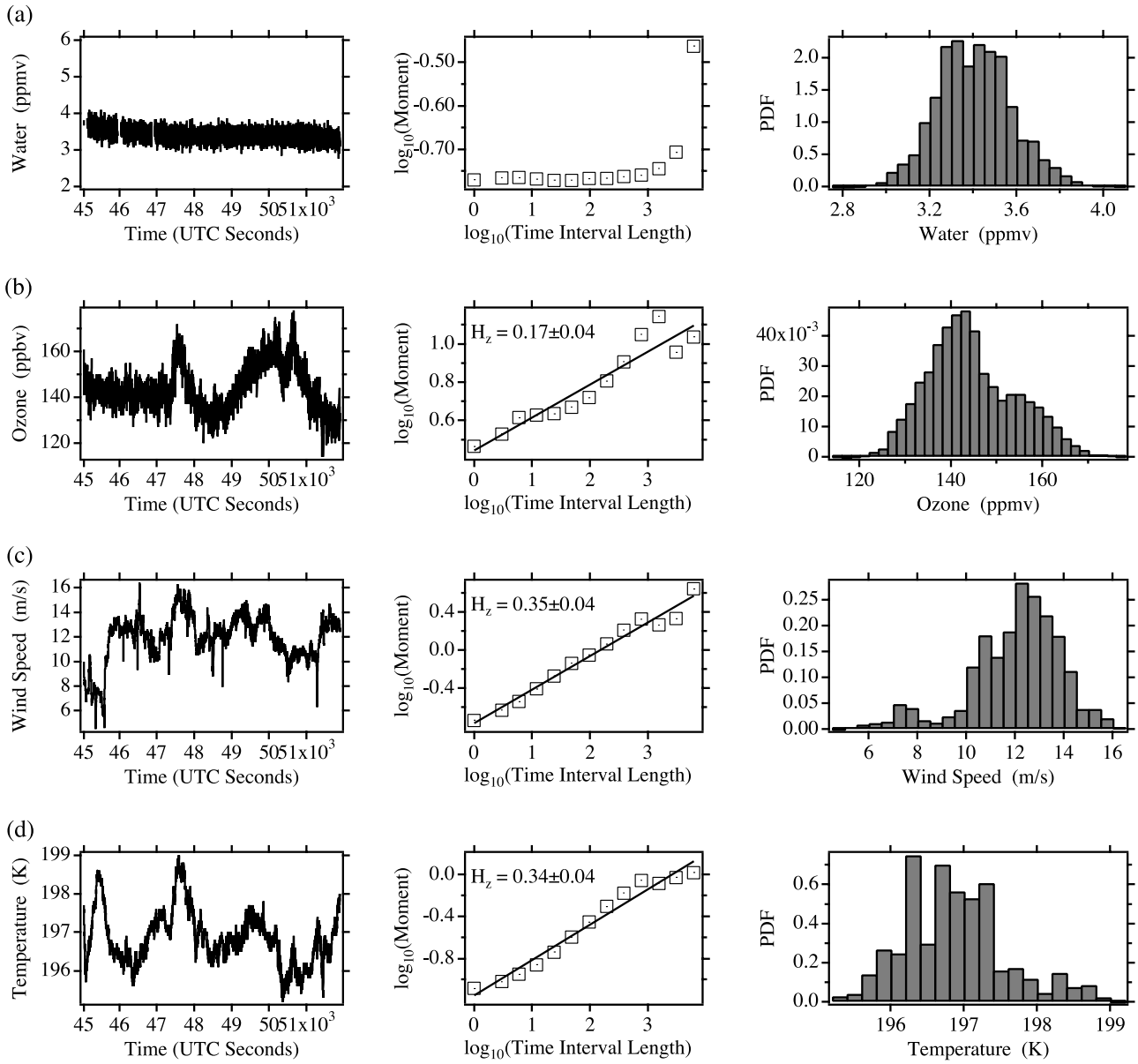

Figure 4. Same as for Figure 1 but for the 6845-s leg of the ER-2 on 14 August 1987.

[10] It has long been known from spectral analysis for the ER-2 that there is a transition between larger scale, atmospheric variability, and "white noise" at some smaller scale, characteristic of the particular variable and the instrument used to measure it [*Murphy*, 1989]. Murphy also pointed out that the meteorological variables, the winds, and the temperature could directly affect the aircraft motion, whereas such observables as water, ozone, and nitrous oxide could not. This leads to our experience in analyzing 10-Hz meteorological data for the ER-2 when flying in Mach cruise mode on stratospheric polar ozone missions. While the aircraft's horizontal motion does scale with ${}^{a}H_z = 1$ (i.e., it is a smooth nonfractal path), the vertical motion is a fractal random walk, showing four regimes. At very small scales, noise in knowledge of the aircraft's motion leads to an ${}^{a}H_z = 0$ region, followed by a region where the aircraft's inertia is such that its motion is unaffected by atmospheric turbulence, where ${}^{a}H_z = 1$. From approximately 3–300 km (15–1500 s flight time) the aircraft trajectory, as the result of autopilot response to atmospheric motion and temperature fields through which it flies, is fractal with ${}^{a}H_z = 5/9$ [*Lovejoy et al.*, 2001; *Tuck et al.*, 2002]. At scales larger than 300 km, ER-2 Mach cruise flight segments have ${}^{a}H_z = 1$ in the vertical, as the result of a steady increase in altitude and of the effect of repeated autopilot corrections aimed at reaching a fixed distant waypoint on the great circle. The net effect is steepening of the aircraft's log-log variogram at the largest scales; combined with the flattening at the smallest scales, a straight fit to the points over the whole range of flight tracks extending up to $O(10^4)$ s will approximate to within ±10% the scaling behavior in the 10^0–10^3 s range. Alternatively, the straight-line fit can be performed over the 10^0–10^3 range; both have been done with similar results (see Table 2). The flight segments we have dealt with here were not performed in Mach cruise mode but rather holding a constant pressure altitude. The

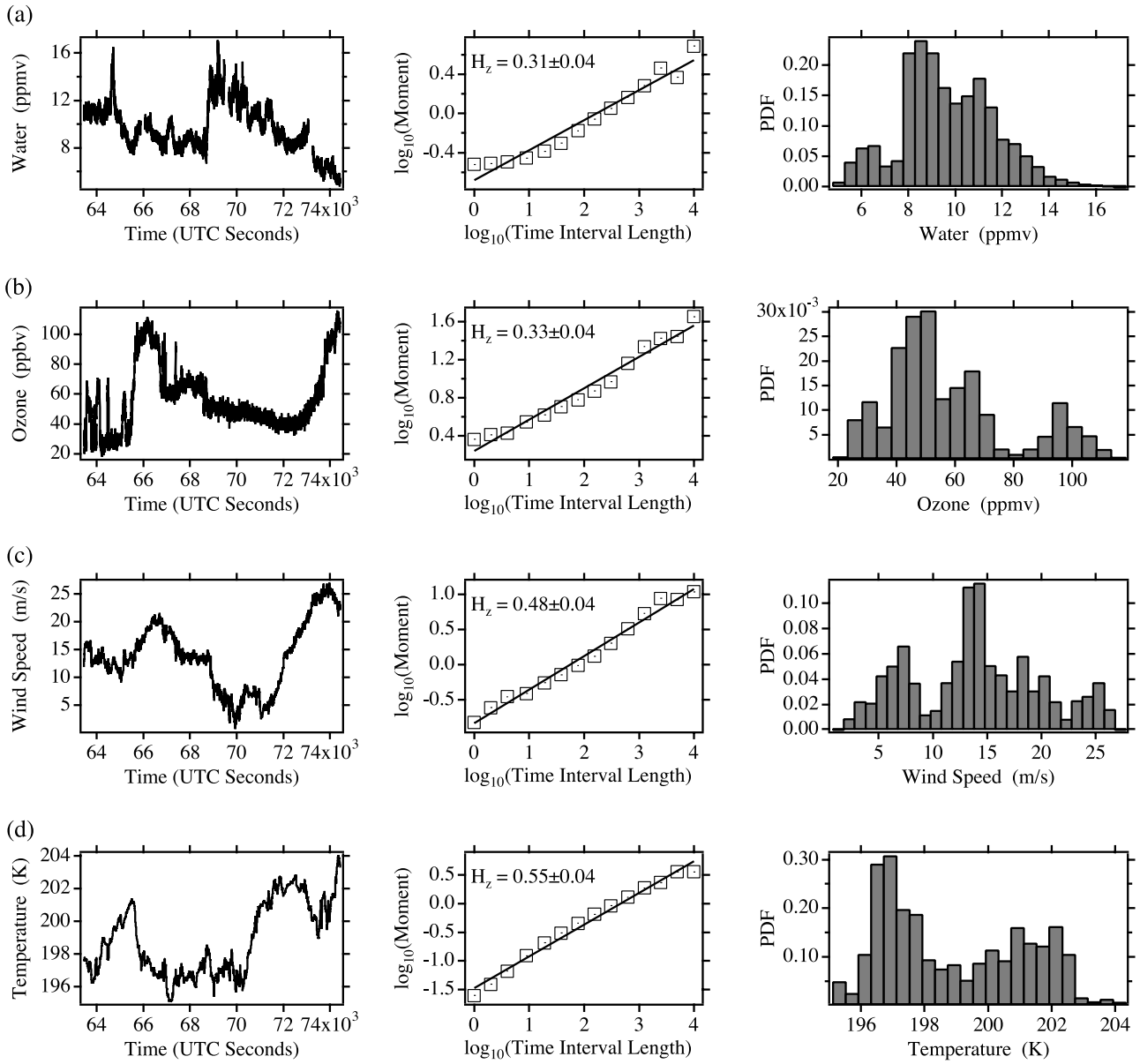

Figure 5. Same as for Figure 1 but for the 10,992-s leg of the WB57F on 21 September 1999.

horizontal coordinates of the aircraft still had ${}^{a}H_z = 1$, and the vertical trajectory was still fractal for the great majority of the flights.

[11] This behavior of the aircraft trajectory is reflected in the variables measured along it. It is especially true of winds and temperature, which are calculated as the vector difference between the aircraft's true airspeed and its ground speed. The best test of the scaling exponents H_z for ozone and water would be to compare them with that of a known passive scalar, rather as O_3, NO_y, and ClO were compared to N_2O in the Arctic stratospheric vortex [*Tuck et al.*, 2002, 2003]. There $H_z(N_2O) = 5/9$, while the others showed very significant deviations from this value, indicating the operation of sources and sinks at a faster rate than mixing. However, in the absence of such a suitable tracer near the tropical tropopause (none have the requisite combination of time response, signal-to-noise ratio, and dynamic range), we can compare $H_z(H_2O)$ and $H_z(O_3)$ to $H_z(T)$ and $H_z([u^2 + v^2]^{1/2})$ over both the full range and over the 10^0–10^3 s range.

[12] An issue for water in the lower stratosphere and for ozone in the upper troposphere is the ratio of the instrument sensitivity to the atmospheric variability. In general, the noise generated by the instrument-aircraft combination is Poissonian or Gaussian, whereas the atmospheric variability is not. We therefore expect a change of slope in the log-log plot for H_z at the time point (horizontal scale) where the amplitudes of the atmospheric variability and the instrumental noise are equal. We justify this interpretation of such scale breaks by adding Gaussian noise, representative of an instrument, to a trace generated by an algorithm known to produce synthetic, scaling data. The H_1 for the synthetic signal and for the synthetic signal plus noise is shown in Figure 2. Note that the instrument noise still affects the scaling at scales greater than the scale break ($\sim\log(t) = 1.2 \approx$ 3 km for Figure 2b, $\sim\log(t) = 1.6 \approx 8$ km for Figure 2c), and

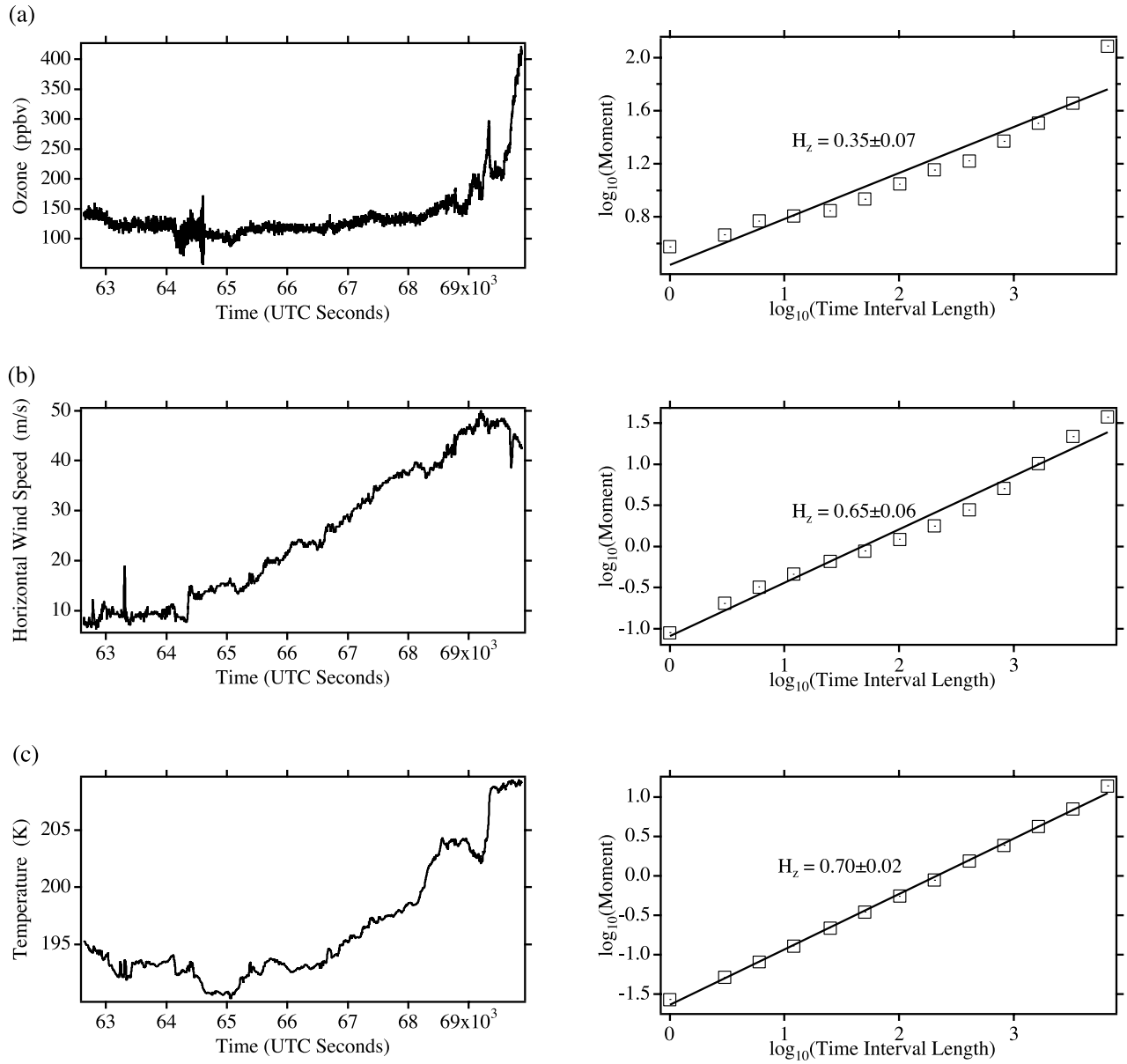

Figure 6. The traces and plots for the estimation of H_z for the same 7242-s segment illustrated in Figure 1. (a) Ozone, (b) wind speed, and (c) temperature.

one cannot therefore use the data to make statements about atmospheric variability on scales larger than this, although the mean mixing ratio does have significance; note, however, that in practice there are many flight legs where this effect is unimportant, since the instrument noise was low enough relative to atmospheric variability. A case where it did matter was for the total water instrument in the lower stratosphere [*Kelly et al.*, 1993] because despite having a total error of only 7%, the very low variability in stratospheric water away from sinks (located mainly near the tropical tropopause and in the Antarctic vortex) meant that little could be deduced about it outside these regions other than via large-scale means. However, the greater abundance of total water in the upper tropical troposphere alleviates this problem there but makes it worse for the ozone instrument, which provided excellent scaling in the stratosphere, for which it was designed, but which had difficulty in the upper tropical troposphere where it recorded abundances in the range 4–130 ppbv. We illustrate the point in Figure 3 with ozone data from a single flight, 11 May 1998, during which upper tropospheric ($\theta \approx 374$ K) and lower stratospheric ($\theta \approx 418$ K) legs were flown. The ozone in the stratospheric segment scales, while the tropospheric one does not. The reverse is true for total water (not shown). We have not computed H_z across sharp scale breaks. Rather, we omit data manifesting sharp scale breaks when considering all scales and only include it when we limit the scales under consideration. Any remaining deviations at the smallest and largest scales are the result of the aircraft motion, as explained above.

3. Results

[13] The values of H_z obtained for each flight segment in Table 1 are displayed for total water, ozone, wind speed, and

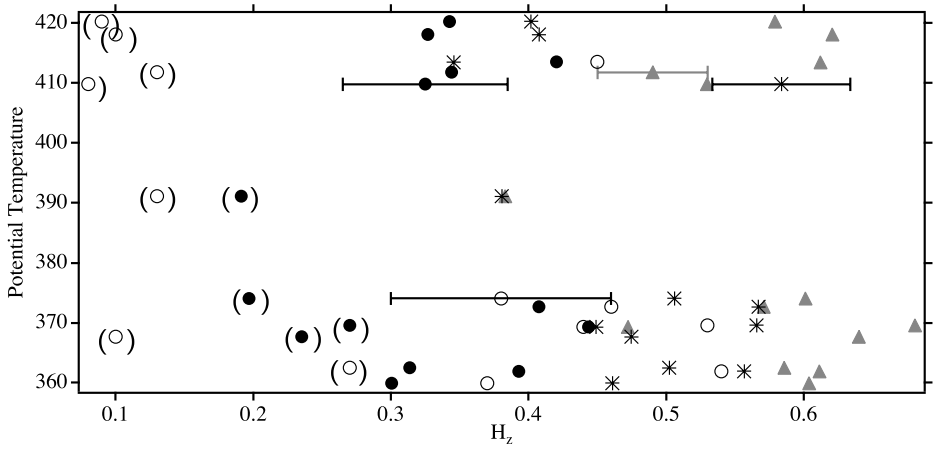

Figure 7. Scaling exponents H_z (abscissa) as a function of potential temperature (ordinate). Open circles, total water; filled circles, ozone; asterisks, wind speed; and shaded triangles, temperature. These data are calculated for the 10^0-10^3 s range; the low values for total water and ozone ($H_z < 0.3$) are the result of instrumental noise and are bracketed. A typical error bar has been added to one point for each of the four variables on the H_z axis. The standard deviation on the potential temperature axis is typically less than 5 K and represents variability along the flight track, not error.

temperature in Table 2; each segment is uniquely identified by its duration in seconds, and the entries are in the same order as in Table 1. Each entry consists of a pair of numbers. The upper number results from fitting a line through all of the points on the log-log plot. A hyphen indicates that there was a sharp scale break due either to instrument noise or to "porpoising" of the aircraft, which results in a sharp scale break at large scales. The lower number results from fitting a line through the points in the range 10^0-10^3 s in the case of ozone, wind speed, and temperature, and from fitting a line from the top end of the instrument noise regime to 10^3 s in the case of total water. We have chosen to interpret the values of $H_z(H_2O)$ thus obtained as characteristic of the atmosphere, a position that can be reevaluated as water instruments with lower noise characteristics become available.

[14] We calculated the intermittency exponents C_1 and the Lévy indices α as in the work of *Tuck et al.* [2002]. The results are consistent with those reported there for the polar vortex and are also consistent with those in the work of *Pecknold et al.* [1993] and are therefore in accord with the unified scaling theory of *Schertzer and Lovejoy* [1987]. The exponents C_1 and α play no further part in the remaining analysis.

[15] The linearity of the log-log plots from which the values in Table 2 were obtained was in general good. The plots for the flight segments of lengths 6845 and 10,992 s are illustrated in Figures 4 and 5 for total water, along with the time series from which they were derived. The probability distributions are also plotted. It is noticeable that where there is very little variability in total water, such as the lower stratospheric 6845 s segment (Figure 4), the value of $H_z(H_2O)$ is undefined because of the lack of scaling. The probability distribution is also Gaussian-like. These characteristics are an indication that for this segment, the water instrument's signal-to-noise ratio at 1 Hz is smaller than the (very low) level of atmospheric variability and that the value of $H_z(H_2O)$ is therefore undefined because of the lack of scaling behavior. It is the equivalent of the flattening to zero slope observed at high frequencies in spectral analysis by *Murphy* [1989]. The water data from 8 of the 14 legs studied were found to have this problem; the water data from the remaining 6 legs are typified by the 10,992-s segment illustrated in Figure 5. In these cases, the water-mixing ratio is larger than the 3–6 ppmv of the five lower stratospheric cases and is also more variable. The scaling is generally similar to that of the ozone. The first-order structure function was evaluated for the data shown in Figures 1, 4, and 5, and the results are plotted in the center log-log plots as the square symbols (log(Moment)). Figure 6 shows the results for ozone, wind speed, and temperature for the 7242-s flight segment. Irrespective of location relative to the tropopause, collectively, the data illustrate that in the range $360 \leq \theta \leq 420$ K there is scale invariance in total water, ozone, wind speed, and temperature, as evidenced by the linearity of the log-log plots [*Schertzer and Lovejoy*, 1987], subject to the discussion in section 2. The invariance extends over flight tracks from 6 to 25 great circle degrees in length, down to a few hundred meters. The associated histograms have long tails.

[16] The values of H_z for total water, ozone, wind speed, and temperature, calculated over the 10^0-10^3 s range, are shown as a function of potential temperature in Figure 7. The respective mean values of H_z are 0.29, 0.32, 0.48, and 0.57 (see last row of Table 2). Note that there are flight segments where the H_z values for ozone and water are significantly less than those for wind speed and temperature. The values are generally in line with expectations from recent analyses of ER-2 data in the lower stratosphere [*Lovejoy et al.*, 2001; *Tuck et al.*, 2002] as regards wind speed and temperature. Both ozone and total water show some evidence ($H_z < 0.55$) that, in some locations throughout the $360 < \theta < 420$ K range in the tropics and subtropics, they are not passive scalars (tracers); this suggests that sources and sinks are operative on timescales faster than mixing. Note that there are some instances where total water and ozone are close to behaving as passive scalars, a

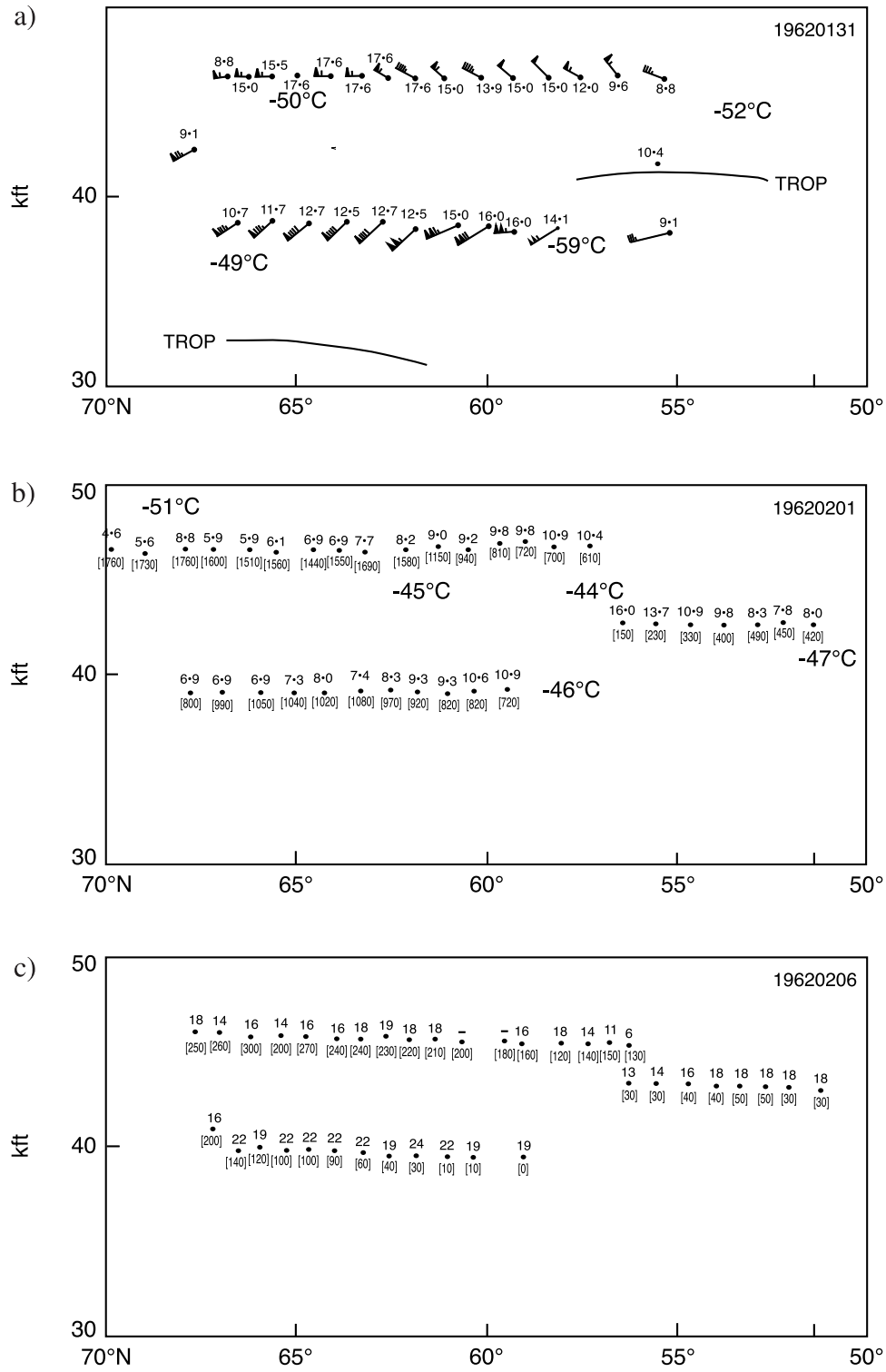

Figure 8. Water vapor and ozone along the Canberra flight track 55°–68°N near the Greenwich meridian. Wind speed and direction are conventional for the fleches; the plain number is water volume mixing ratio in ppmv, that in square brackets is ozone, ppbv. (a) 31 January 1962, (b) 1 February 1962, and (c) 6 February 1962. All flights were approximately centered in local noon.

reasonable condition if there has been no recent precipitation or photochemistry, respectively. There is no conclusive evidence for any systematic change in any exponent for any variable as a function of potential temperature in the 60-K range, which includes the tropical tropopause, although H_z for wind speed and temperature tends to be higher at the lower potential temperatures ($360 < \theta < 370$ K). The reason for this appears to be the large-scale wind shear and

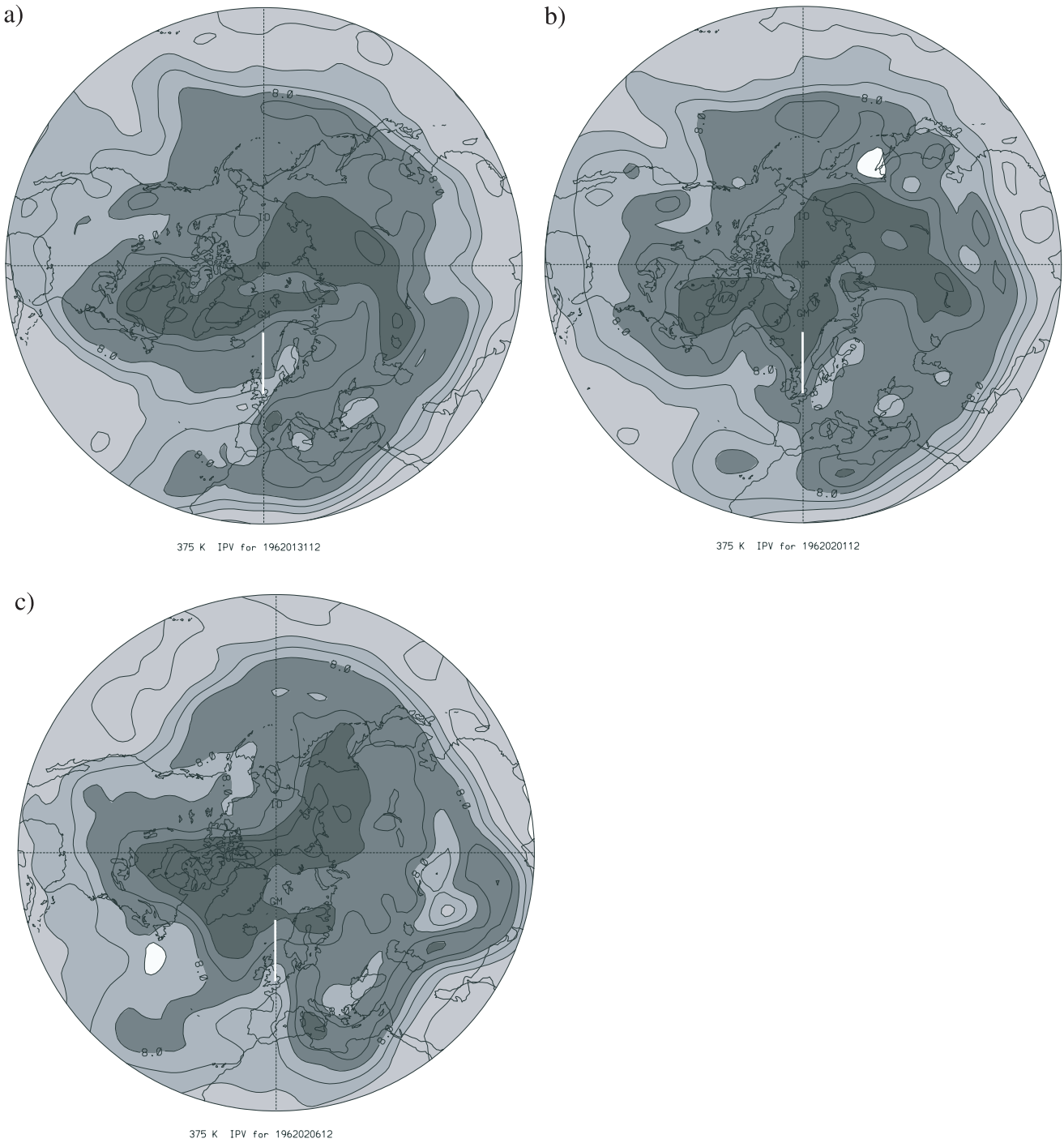

Figure 9. Potential vorticity maps for 12 UTC at $\theta = 375$ K corresponding to the three 1962 Canberra flights in Figure 8. The 8.0 contour is labeled. The contour interval is 2.0. The flight track is indicated by the white line segment running from 51° to 68°N along the Greenwich meridian. It may be seen that the (a) 31 January 1962 and (c) 6 February 1962 flights correspond to incursions of low-PV air into the subarctic from the subtropics, whereas that of (b) 1 February 1962 corresponds to an incursion of high-PV (vortex) air over the Bay of Biscay. The former have air like that seen by the ER-2 and WB57F in Figures 10 and 11, while the latter has high ozone and low water characteristic of older air descended from the middle stratosphere.

temperature gradient in the subtropical jet stream, which has its maximum strength at these potential temperatures and which often had its core of high wind speed near the WB57F base at Ellington Field (30°N, 95°W). This interesting correlation, which may portend a link between unified scale invariance and traditional large-scale dynamical meteorology, cannot be pursued further here. Analysis of the much larger number of flights available across the

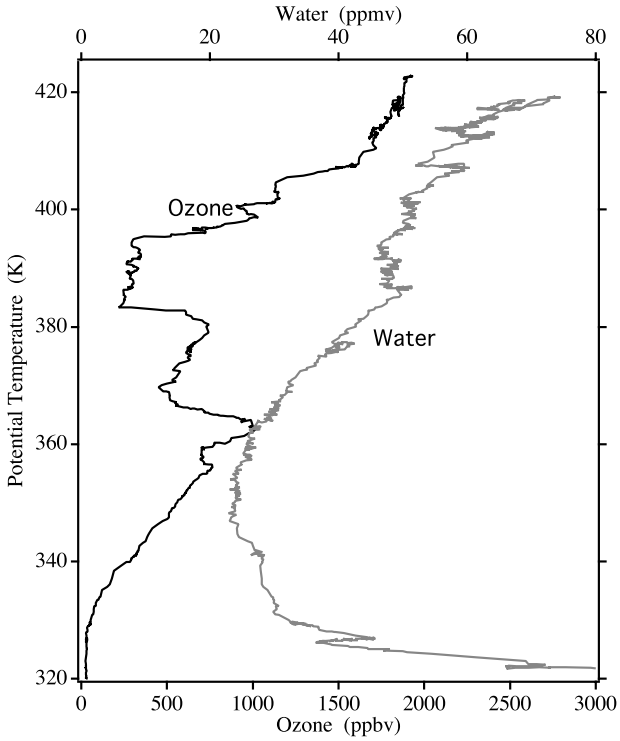

Figure 10. Profiles of water and ozone, following ER-2 take-off from Stavanger (59°N, 6°E) on 7 February 1989. Note the values of ozone and water at $\theta \leq 420$ K. The tropopause was at $\theta = 330$ K. These data were not used in Table 2 or the scale analysis.

stratospheric polar night jet stream establishes it as a statistically significant phenomenon there.

4. Large-Scale Context of Past and Present Observations

[17] There have been consistent reports of high, >10 ppmv and up to 80 ppmv on occasion, episodic values of water vapor above the tropopause in midlatitudes of the Northern Hemisphere during Meteorological Research Flight Canberra operations, detected as excursions from sequences of more frequent, lower values [*Helliwell et al.*, 1957; *Cluley and Oliver*, 1979; *Foot*, 1984]. A similar record exists for a balloon-borne frostpoint hygrometer, which normally recorded low values [*Mastenbrook*, 1968]. There is one account [*Roach*, 1962] of values of water >10 ppmv and of ozone in the range $100 < O_3 < 1500$ ppbv well above the tropopause on the Canberra flight track from 50° to 68°N near the Greenwich meridian on 6 February 1962. In Figure 8, we redraw those observations along with the flights of 31 January 1962 and 1 February 1962, with units of ppmv for water and ppbv for ozone. All three are in the range 350–390 K and are above the tropopause. The flight of 1 February 1962 has low water and high ozone, unequivocally stratospheric characteristics. The other two however show upper tropospheric water and low but stratospheric ozone.

[18] The NOAA-NCEP reanalyzed potential vorticity maps for the Meteorological Research Flight Canberra flights on 31 January 1962 and 6 February 1962 similarly confirm the subtropical origin, in this case from the Mexican Gulf and Atlantic sectors, respectively (Figure 9). By contrast, the potential vorticity (PV) map for 1 February 1962 shows the polar vortex extending south along the Greenwich meridian to the Bay of Biscay, explaining the low water, high ozone air seen by the aircraft; it was flying in the highest PV air in the whole vortex on its track along the Greenwich meridian to 68°N.

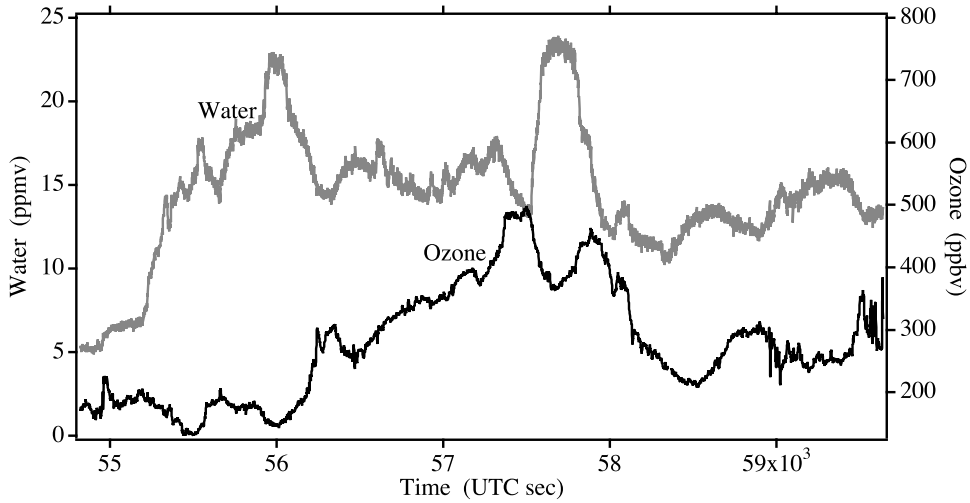

Figure 11. A segment from the WB57F flight of 6 May 1998. The ozone and water traces were taken just above the tropopause, on the cyclonic side of the subtropical jet stream core. The joint distribution of water (10–15 ppmv) and ozone (200–500 ppbv) is evidence of mixing of upper tropospheric and lower stratospheric air; the air is in the stratosphere. These data were not used in Table 2 or the scale analysis.

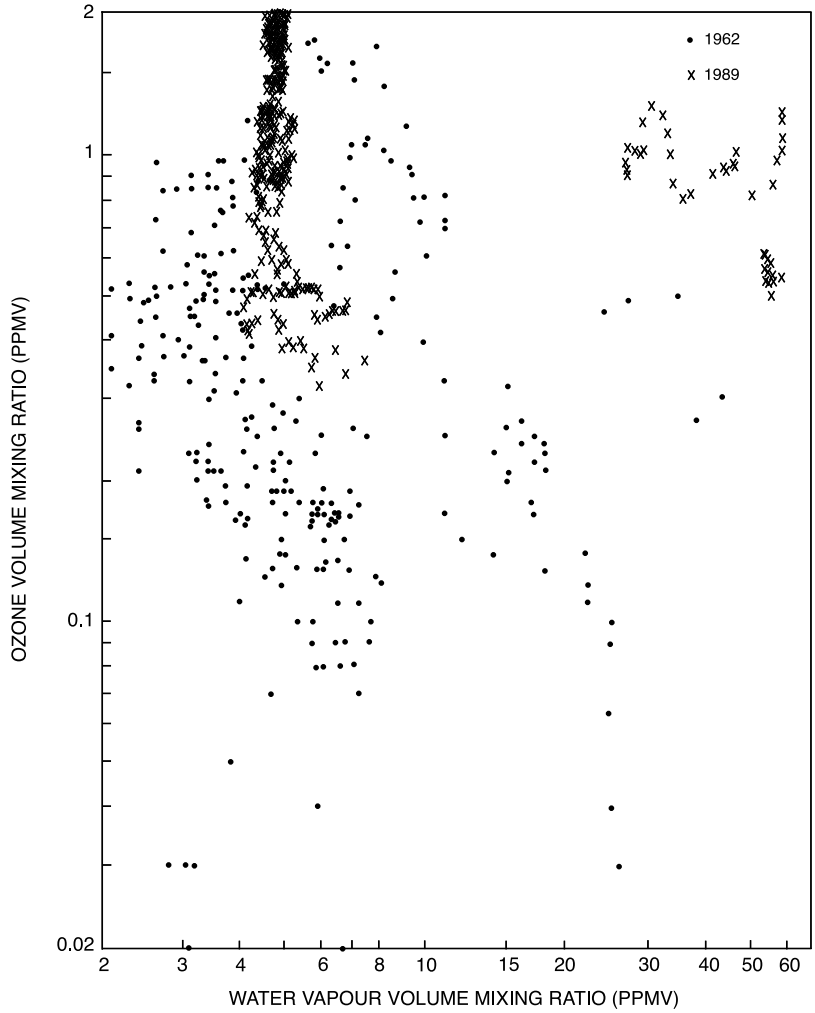

Figure 12. An ozone-water scatterplot, modified and extended from *Roach* [1962, Figure 3]. Only the stratospheric points have been retained; points have been added from three ER-2 flights in January–February 1989 taken when the vortex was undisturbed (6, 12, and 16 January1989) and from one flight when it was disturbed (7 February 1989). All points in the range $350 < \theta < 400$ K have been plotted. Dots represent 1962; crosses represent 1989; the high water points correspond to disturbed conditions in each case. Note that the abscissa is logarithmic; the disturbed 1962 points have significantly more water than those taken in undisturbed conditions.

[19] The ER-2 flight of 7 February 1989 (Figure 10), some 27 years later, shows a similar population characterizing air in the range $340 < \theta < 420$ K as having stratospheric ozone (100–1000 ppbv) accompanied by upper tropospheric water (up to 25 ppmv) near 60°N, 6°E. Such air can only have been obtained by mixing between lower stratospheric and upper tropospheric elements; grand averages over scores of vertical profiles by the ER-2 between 1987 and 1996 reveal this to be the case [*Reid et al.*, 2000]. Back trajectories using the NOAA-NCEP reanalysis from the ER-2 flight of 7 February 1989 confirm that air on the cyclonic side of the subtropical jet stream over North Africa moved, after circling the globe once in 5 days, to be above Stavanger at the time of the observations in Figure 10. We note that the section of WB57F flight on 6 May 1998 shown in Figure 11 was flown above the tropopause at latitudes immediately north from the subtropical jet stream core and contains air with ~300 ppbv of ozone accompanied by ~15 ppmv of water; these simultaneous values can only have occurred via the mixing of tropospheric and stratospheric air.

[20] Points from three ER-2 flights from January 1989 over Scandinavia during undisturbed conditions are plotted with those from the disturbed flight of 7 February 1989 and the three 1962 Canberra flights in Figure 12. It should be noted that the 1962 data are considerably less accurate than those from 1989, but that the 1962 points during disturbed conditions are nevertheless significantly separate from those in undisturbed conditions, in the sense of combining high-water and high-ozone mixing ratios. The presence of air with upper tropospheric water and lower stratospheric ozone is evident during disturbed conditions in both 1962 and 1989 and is similarly absent from the vortex or near-vortex air encountered in undisturbed conditions in both years. It is interesting to note, therefore, that the intrusions of upper tropical tropospheric air into the Northern Hemisphere lower stratosphere in the Atlantic sector [*Reid et al.*, 2000] are correlated with distortions of the edge of the Arctic vortex. Of course,

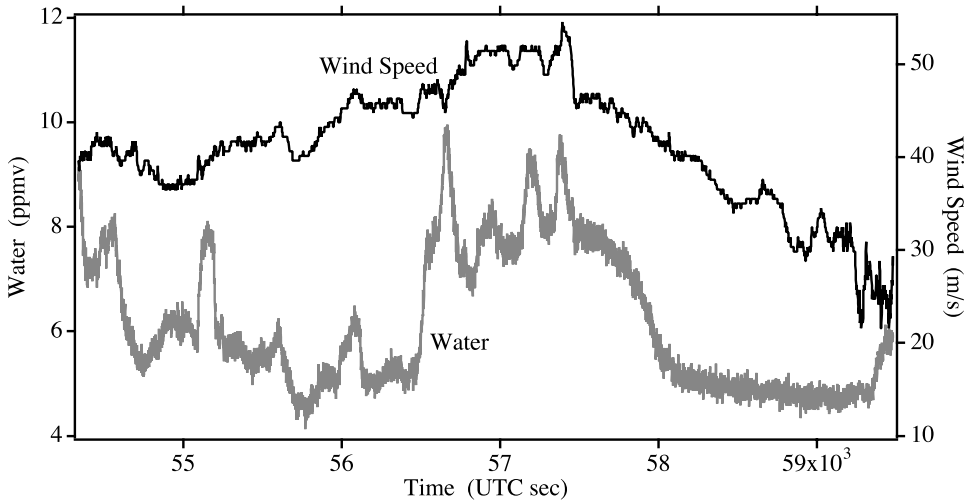

Figure 13. Water and wind speed from the WB57F track on 7 May 1998, flown isentropically at 370 K. The cross section is on a line running from the right entrance toward the left exit of the subtropical jet stream maximum over the southern United States. Note the absence of a sharp, spatially confined gradient in the mixing ratio of water; there is a mixing slope between 57,400 and 59,000 s and considerable interleaving of tropospheric and stratospheric mixing ratios at earlier times.

PV maps cannot resolve much of the fine scale structure evident in the 1989 aircraft data, and the lower frequency and lower accuracy of the 1962 aircraft data are also impediments during those flights 27 years earlier.

[21] The presence of air containing lower stratospheric ozone and upper tropospheric water on the immediately cyclonic side of the subtropical jet stream on 6 May 1998 (Figure 11) thus confirms the validity of the earlier measure-

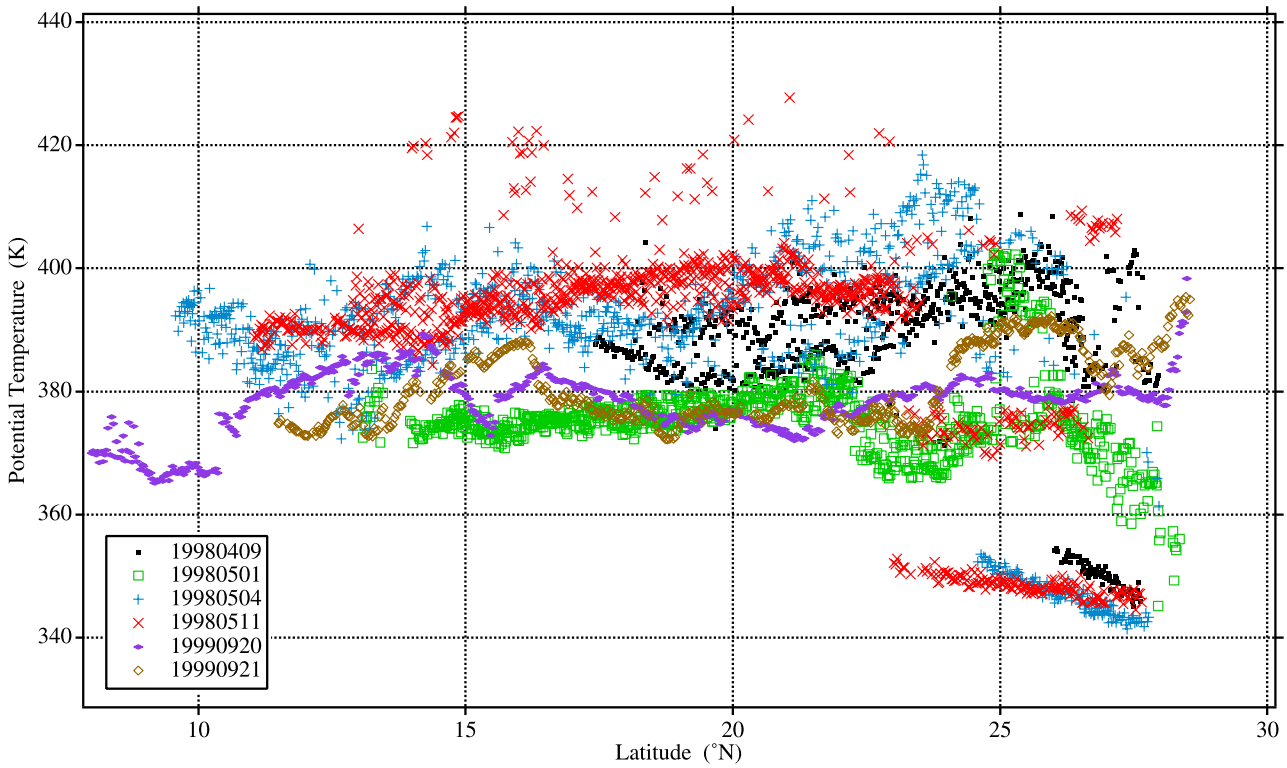

Figure 14. A scatterplot of the potential temperature at the tropopause, θ_T, versus latitude for the WB57F flights of 9 April 1998, 1, 4, and 11 May 1998, and 20 and 21 September 1999. Note that for each flight θ_T is higher at the latitudes nearer the subtropical jet stream (i.e., further from the equator), and that θ_T is greater in spring than in fall. Some flights show a much lower midlatitude tropopause underlying the higher tropical tropopause at latitudes poleward of 23°N.

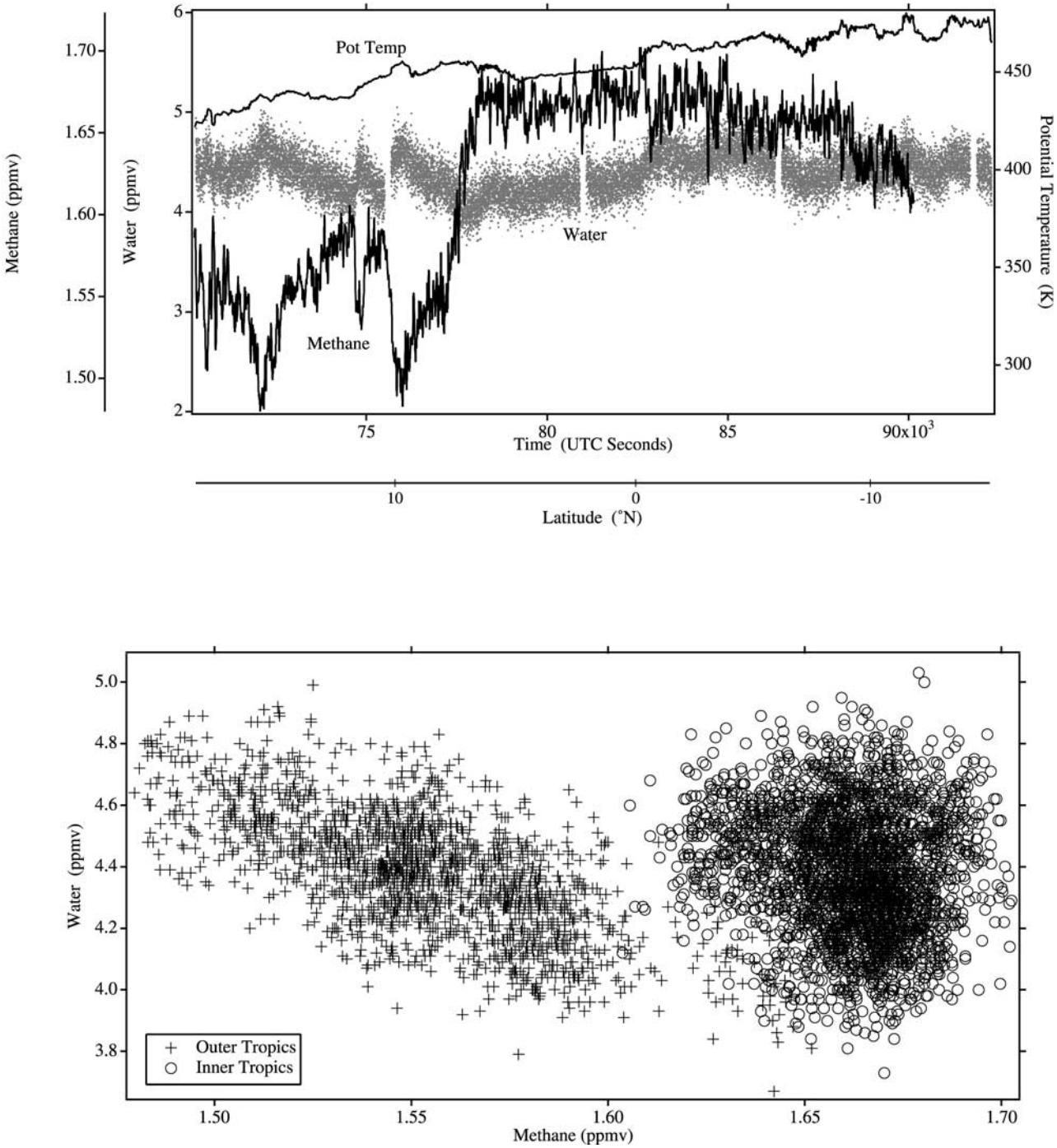

Figure 15. Water and methane measurements from the ER-2 flight of 27 March 1994, between Hawaii (20°N, 158°W) and Fiji (18°S, 177°E). Even at $\theta > 440$ K, in the inner tropics the water is variable and is uncorrelated with methane. There is a mixing slope in the methane trace between 8° and 10°N in the upper frame and overlap between 1.60 and 1.66 ppmv CH_4 on the scatterplot in the lower frame. These data were not used in Table 2 or the scale analysis.

ments and directly shows the subtropical jet stream to be a mixing and exchange zone, as proposed by *Brewer* [1960], *Murgatroyd* [1965], *Allam and Tuck* [1984], *Foot* [1984], *Dessler et al.* [1995], and *Tuck et al.* [1997]. This view is reinforced by the 5144-s segment flown by the WB57F on 7 May 1998. The flight track was diagonally across the subtropical jet stream as a segment of a line running from the right entrance toward the left exit, isentropically at 370 K. Figure 13 shows the wind speed and water traces; consistent with the scale invariance in both (row 9 of Table 2), there is substantial variability on all scales. It is clear from the water that there is exchange across the core; there is a mixing slope region and interleaving of air filaments with higher and lower water mixing ratios. Recent work [*Vaughan and Timmis*, 1998; *O'Connor et al.*, 1999; *Reid et al.*, 2000] has shown explicit examples of such

transport from the subtropical jet region to midlatitudes in the context of Lagrangian and PV analyses from global numerical weather prediction suites. The long-tailed distributions seen by *Helliwell et al.* [1957] and *Mastenbrook* [1968] in lower stratospheric frost point observations are consistent with the analysis; such probability distribution functions have been shown to be an adjunct of scale-invariant (fractal) behavior by *Schertzer and Lovejoy* [1985], *Dewey* [1997], *Turcotte* [1997], *Mandelbrot* [1998], and *Malamud and Turcotte* [1999].

5. Discussion and Conclusions

[22] Flights in the range $360 < \theta < 420$ K at latitudes in the band from 18°S to 33°N have shown fractal behavior, with the concomitant scale invariance and long-tailed probability distributions in ozone, total water, wind speed, and temperature. The range of potential temperatures spans the scale height centered on the tropical and subtropical tropopause; Figure 14 shows a scatterplot of the tropopause potential temperature θ_T versus latitude for selected flights, which are typical of all flights. The remarkable feature that for each individual flight θ_T is lower near the equator and higher near the subtropical jet stream by 10–20 K (typically 365–395 K in the inner tropics, 370–420 K on the immediate anticyclonic side of the jet maximum) reflects the transport of potentially warm air from the lower midlatitude stratosphere along the up-sloping isentropes toward and into the inner tropics. Such motion will also tend to destabilize the air with respect to vertical air parcel motion [*Haltiner and Martin*, 1957] and so tend to raise the tropopause. The measurements of ozone, methane (Figure 15), and water are consistent with such air motion, with mixing ratios showing transport from middle to lower latitudes. There is considerable overlap of the two populations on the scatterplot in the upper half of the figure, which is manifest as a mixing slope in the methane trace from 1.67 to 1.49 ppmv, centered at 8°N, in the lower half. In all cases, including the inner tropics, the tropopause is at a higher value of potential temperature than that equivalent to the highest observed moist static energies θ_W at the tropical surface, some 355 K. The $\theta_T - \theta_W$ is larger (up to 40 K) in spring than in the fall (about 10 K), indicating that there is more adiabatic transport of potentially warm air from midlatitudes during the earlier season. This is consistent with the tracer structure discussed in the work of *Tuck et al.* [1997] and shown for methane and water in Figure 15.

[23] The scale invariance specifies the statistical distributions involved and generated when stratosphere-troposphere exchange and mixing occur along the tropical tropopause and at the horizontal boundary formed by the subtropical jet stream; the associated probability distributions show the expected long tails. Figure 15 shows the behavior of methane and water during a long flight from Hawaii (20°N, 158°W) to Fiji (18°S, 178°E) at $440 < \theta < 470$ K. In the inner tropics, there is no correlation between methane and water, with the latter varying in a range of 1.3 ppmv centered on a mean of 4.3 ppmv; there is no clear one-to-one relationship well above the inner tropical tropopause. Comparatively rare, relatively intense events may have substantial influence as expected from the long-tailed distributions, and accordingly, a unique mapping of the total hydrogen content crossing the tropopause on to the content of the "overworld" (the stratosphere above about 50 hPa in the tropics and above about 100 hPa in the extratropics) should not be expected. Instead, it is determined by the interplay of subtropical jet stream dynamics and inner tropical ascent via deep convection over the annual cycle in the range $360 < \theta < 450$ K, with whatever their resultant is at about 50–60 hPa in the inner tropics being the content of what enters the overworld. There is no single "entry level" value of total hydrogen at the tropical tropopause. Note that despite this there is a "tape recorder" signal of the effects of the annual cycle [*Mote et al.*, 1996]; the "head" is however at 50–60 hPa, not at 90–100 hPa. Recirculation [*Tuck et al.*, 1997] and the intrusion of upper tropospheric tropical air into the lower midlatitude stratosphere [*Reid et al.*, 2000], working through the dynamics associated with the subtropical jet stream, are in evidence in the "middleworld"; there is a further implication that interpreting observed trends in stratospheric water and methane will not be as simple as diagnosing tropopause temperature. *Rosenlof* [2002] has come to similar conclusions in analyzing satellite data in conjunction with meteorological assimilations. Scale invariance implies participation of all scales in mixing and exchange and that relatively infrequent but high-amplitude events contribute substantially to the maintenance of the mean state. Events of all scales which mix or cool air near the tropical tropopause to frost point have the potential to influence stratospheric water content, and their weighting will be described by long-tailed probability distributions. These fat-tailed distributions and associated scale invariance for upper tropical tropospheric water and ozone have consequences for the notion of a cascade of fluid mechanical energy from the largest, input scales to the smallest, dissipative scales. Since both species absorb and emit infrared radiation, and both absorb solar radiation, and moreover are at least sometimes not passive scalars, such a fluid mechanical cascade cannot be conservative; radiative energy is input and dissipated by water and ozone on all scales, affecting the temperature and hence the turbulence. Such a conclusion has implications for the simulation of both atmospheric dynamics and climate, particularly in view of the fact [*Doherty and Newell*, 1984] that the upper troposphere is the altitude range where many of the most important water vapor infrared absorption bands change from being self-absorbed below to transparent above.

[24] The number of flights in the upper tropical troposphere is far less than is available for the polar vortex and midlatitudes. It is clear that better definition and understanding of the exponents quantifying generalized scale invariance in the observationally challenging upper tropical troposphere could be obtained if (1) there were more flights, (2) there were higher-frequency observations, and (3) the observations had better signal-to-noise ratios and fewer data gaps. Some or all of these desiderata are feasible.

[25] **Acknowledgments.** We thank G. Kiladis for Figure 9, C. R. Webster for the methane data in Figure 15, and R. Herman for the water data on the 26 July 2002 flight segment. Work performed by M. J. Mahoney at the Jet Propulsion Laboratory, California Institute of Technology, was carried out under contract with the National Aeronautics and Space Administration. Constructive criticism of the original manuscript and the revision by an anonymous referee clarified the paper.

References

Allam, R. J., and A. F. Tuck, Transport of water vapour in a stratosphere-troposphere general circulation model, II, Trajectories, *Q. J. R. Meteorol. Soc.*, *110*, 357–392, 1984.

Brewer, A. W., Evidence for a world circulation provided by measurements of the helium and water vapour distribution in the stratosphere, *Q. J. R. Meteorol. Soc.*, *75*, 351–363, 1949.

Brewer, A. W., The transfer of atmospheric ozone into the troposphere, MIT Planetary Circulation Project, paper presented at the United Nations Committee on the Effects of Radiation (UNSCEAR), Mass. Inst. of Technol., New York, Jan. 1960.

Cluley, A. P., and M. J. Oliver, An observation of unusually high humidity in the stratosphere, *Q. J. R. Meteorol. Soc.*, *105*, 306–309, 1979.

Danielsen, E. F., In situ evidence of rapid, vertical, irreversible transport of lower tropospheric air into the lower tropical stratosphere by convective cloud turrets and by larger scale upwelling in tropical cyclones, *J. Geophys. Res.*, *98*, 8665–8681, 1993.

Denning, R. F., S. L. Guidero, G. S. Parks, and B. L. Gary, Instrument description of the airborne Microwave Temperature Profiler, *J. Geophys. Res.*, *94*, 16,757–16,766, 1989.

Dessler, A. E., A reexamination of the "stratospheric fountain" hypothesis, *Geophys. Res. Lett.*, *25*, 4165–4168, 1998.

Dessler, A. E., E. J. Hintsa, G. M. Weinstock, J. G. Anderson, and K. R. Chan, Mechanisms controlling water vapor in the lower stratosphere: "A tale of two stratospheres", *J. Geophys. Res.*, *100*, 23,167–23,172, 1995.

Dethof, A., A. O'Neill, J. M. Slingo, and H. G. J. Smit, A mechanism for moistening the lower stratosphere involving the Asian summer monsoon, *Q. J. R. Meteorol. Soc.*, *125*, 1079–1106, 1999.

Dewey, T. G., *Fractals in Molecular Biophysics*, chap. 4.1, Oxford Univ. Press, New York, 1997.

Doherty, G. M., and R. E. Newell, Radiative effects of changing stratospheric water vapour, *Tellus, Ser. B*, *36*, 149–162, 1984.

Dunkerton, T. J., Evidence of meridional motion in the summer lower stratosphere adjacent to monsoon regions, *J. Geophys. Res.*, *100*, 16,675–16,888, 1995.

Etkin, B., *Dynamics of Atmospheric Flight*, chap. 13, John Wiley, New York, 1972.

Foot, J. S., Aircraft measurements of the humidity in the lower stratosphere from 1977 to 1980 between 45°N and 65°N, *Q. J. R. Meteorol. Soc.*, *110*, 303–319, 1984.

Gage, K. S., J. R. McAfee, D. A. Carter, W. L. Ecklund, A. C. Riddle, G. C. Reid, and B. B. Balsley, Long-term mean vertical motion over the tropical Pacific: Wind-profiling Doppler radar measurements, *Science*, *254*, 1771–1773, 1991.

Haltiner, G. J., and F. L. Martin, *Dynamical and Physical Meteorology*, chap. 5–4, McGraw-Hill, New York, 1957.

Helliwell, N. C., J. R. Mackenzie, and M. J. Kerley, Some further observations from aircraft of frost point and temperature up to 50,000 ft., *Q. J. R. Meteorol. Soc.*, *83*, 257–262, 1957.

Jensen, E. J., O. B. Toon, H. B. Selkirk, J. D. Spinhirne, and M. R. Schoeberl, On the formation and persistence of subvisible cirrus clouds near the tropical tropopause, *J. Geophys. Res.*, *101*, 21,361–21,375, 1996.

Johnston, H. S., and S. Solomon, Thunderstorms as a possible micrometeorological sink for stratospheric water, *J. Geophys. Res.*, *84*, 3155–3158, 1979.

Kelly, K. K., M. H. Proffitt, K. R. Chan, M. Loewenstein, J. R. Podolske, S. E. Strahan, J. C. Wilson, and A. L. Schmeltekopf, Water vapor and cloud water measurements over Darwin during the STEP 1987 tropical mission, *J. Geophys. Res.*, *98*, 8713–8724, 1993.

Lovejoy, S., D. Schertzer, and J. D. Stanway, Direct evidence of multifractal cascades from planetary scales down to 1 km, *Phys. Rev. Lett.*, *86*, 5200–5203, 2001.

Malamud, B. D., and D. L. Turcotte, Self-affine time series, I, Generation and analyses, *Adv. Geophys.*, *40*, 1–90, 1999.

Mandelbrot, B. B., *Fractals and 1/f Noise*, chap. N15, Springer-Verlag, New York, 1998.

Mastenbrook, H. J., Water vapor distribution in the stratosphere and high troposphere, *J. Atmos. Sci.*, *28*, 1495–1501, 1968.

Mote, P. W., K. H. Rosenlof, M. E. McIntyre, E. S. Carr, J. C. Gille, J. R. Holton, J. S. Kinnersley, H. C. Pumphrey, J. M. Russell III, and J. W. Waters, An atmospheric tape recorder: The imprint of tropical tropopause temperatures on stratospheric water vapor, *J. Geophys. Res.*, *101*, 3989–4006, 1996.

Murgatroyd, R. J., Ozone and water vapour in the upper troposphere and lower stratosphere, in *Meteorological Aspects of Atmospheric Radioactivity*, *169*, pp. 68–94, World Meteorol. Organ, Geneva, 1965.

Murphy, D. M., Time offsets and power spectra of the ER-2 dataset from the 1987 Airborne Antarctic Ozone Experiment, *J. Geophys. Res.*, *94*, 16,737–16,748, 1989.

Newell, R. E., and S. Gould-Stewart, A stratospheric fountain?, *J. Atmos. Sci.*, *38*, 2789–2796, 1981.

O'Connor, F. M., G. Vaughan, and H. de Backer, Observation of subtropical air in the European midlatitude lower stratosphere, *Q. J. R. Meteorol. Soc.*, *125*, 2965–2986, 1999.

Pecknold, S., S. Lovejoy, D. Schertzer, C. Hooge, and J. F. Malouin, The simulation of universal multifractals, in *Cellular Automata: Prospects in Astrophysical Applications*, edited by J. M. Perdang and A. Lejeune, pp. 228–267, World Sci., River Edge, N. J., 1993.

Potter, B. E., and J. R. Holton, The role of monsoon convection in the dehydration of the lower stratosphere, *J. Atmos. Sci.*, *52*, 1034–1050, 1995.

Reid, S. J., A. F. Tuck, and G. Kiladis, On the changing abundance of ozone minima in midlatitudes, *J. Geophys. Res.*, *105*, 12,169–12,180, 2000.

Roach, W. T., Aircraft observations in the lower sub-arctic stratosphere in winter, Meteorological Research Committee Paper (MRCP) 121, Natl. Meteorol. Libr., Meteorol. Off., Bracknell, UK, 1962.

Rosenlof, K. H., Transport changes inferred from HALOE water and methane measurements, *J. Meteorol. Soc. Jpn.*, *80*, 831–848, 2002.

Rosenlof, K. H., A. F. Tuck, K. K. Kelly, J. M. Russell III, and M. P. McCormick, Hemispheric asymmetries in water vapor and inferences about transport in the lower stratosphere, *J. Geophys. Res.*, *102*, 13,213–13,234, 1997.

Rosenlof, K. H., et al., Stratospheric water vapor increases over the past half-century, *Geophys. Res. Lett.*, *28*, 1195–1199, 2001.

Schertzer, D., and S. Lovejoy, The dimension and intermittency of atmospheric dynamics, in *Turbulent Shear Flows*, vol. 4, pp. 7–33, Springer-Verlag, New York, 1985.

Schertzer, D., and S. Lovejoy, Physical modeling and analysis of rain and clouds by anisotropic scaling multiplicative processes, *J. Geophys. Res.*, *92*, 9693–9714, 1987.

Seuront, L., F. Schmitt, Y. Lagadeuc, D. Schertzer, and S. Lovejoy, Universal multifractal analysis as a tool to characterize multiscale intermittent patterns: Example of phytoplankton in turbulent coastal waters, *J. Plankton Res.*, *21*, 877–922, 1999.

Sherwood, S. C., A stratospheric "drain" over the maritime continent, *Geophys. Res. Lett.*, *27*, 677–680, 2000.

Simmons, A. J., A. Untch, C. Jakob, P. Kållberg, and P. Unden, Stratospheric water vapour and tropical tropopause temperatures in ECMWF analyses and multi-year simulations, *Q. J. R. Meteorol. Soc.*, *125*, 353–386, 1999.

Sparling, L. C., Statistical perspectives on stratospheric transport, *Rev. Geophys.*, *38*, 417–436, 2000.

Tuck, A. F., and S. J. Hovde, Fractal behavior of ozone, wind and temperature in the lower stratosphere, *Geophys. Res. Lett.*, *26*, 1271–1274, 1999a.

Tuck, A. F., and S. J. Hovde, An examination of stratospheric aircraft data for small scale variability and fractal character, in *Mesoscale Processes in the Stratosphere, Air Pollut. Res. Rep. 69, EUR 18912 EN*, pp. 249–254, Directorate-General Science, Research and Development, European Commission, Brussels, 1999b.

Tuck, A. F., et al., The Brewer-Dobson circulation in the light of high altitude in situ aircraft observations, *Q. J. R. Meteorol. Soc.*, *123*, 1–69, 1997.

Tuck, A. F., S. J. Hovde, and M. H. Proffitt, Persistence in ozone scaling under the Hurst exponent as an indicator of the relative rates of chemistry and fluid mechanical mixing in the stratosphere, *J. Phys. Chem. A*, *103*, 10,445–10,450, 1999.

Tuck, A. F., S. J. Hovde, E. C. Richard, D. W. Fahey, and R. S. Gao, A scaling analysis of ER-2 data in the inner Arctic vortex during January–March 2000, *J. Geophys. Res.*, *107*(D5), 8306, doi:10.1029/2001JD000879, 2002. [Printed in *J. Geophys. Res. 108*(D5), March 2003]

Tuck, A. F., S. J. Hovde, R.-S. Gao, and E. C. Richard, Law of mass action in the Arctic lower stratospheric polar vortex January–March 2000: ClO scaling and the calculation of ozone loss rates in a turbulent fractal medium, *J. Geophys. Res.*, *108*(D15), 4451, doi:10.1029/2002JD002832, 2003.

Turcotte, D. L., *Fractals in Geology and Geophysics*, 2nd ed., Cambridge Univ. Press, New York, 1997.

Vaughan, G., and C. Timmis, Transport of near tropopause air into the lower midlatitude stratosphere, *Q. J. R. Meteorol. Soc.*, *124*, 1559–1578, 1998.

S. J. Hovde, K. K. Kelly, E. C. Richard, T. L. Thompson, and A. F. Tuck, Aeronomy Laboratory, National Oceanic and Atmospheric Administration, R/AL6, 325 Broadway, Boulder, CO 80305-3328, USA. (atuck@al.noaa.gov)

M. J. Mahoney, Jet Propulsion Laboratory, California Institute of Technology, Pasadena, CA 91109-8099, USA.

M. H. Proffitt, World Meteorological Organization, Geneva, CH-1211, Switzerland.